

Tectonics, Dynamics, and Seismic Hazard in the Canada–Alaska Cordillera

Stephane Mazzotti, Lucinda J. Leonard, Roy D. Hyndman, and John F. Cassidy

Geological Survey of Canada, Natural Resources Canada, Sidney, British Columbia, Canada

School of Earth and Ocean Science, University of Victoria, Victoria, British Columbia, Canada

The North America Cordillera mobile belt has accommodated relative motion between the North America plate and various oceanic plates since the early Mesozoic. The northern half of the Cordillera (Canada–Alaska Cordillera) extends from northern Washington through western Canada and central Alaska and can be divided into four tectonic domains associated with different plate boundary interactions, variable seismicity, and seismic hazard. We present a quantitative tectonic model of the Canada–Alaska Cordillera based on an integrated set of seismicity and GPS data for these four domains: south (Cascadia subduction region), central (Queen Charlotte–Fairweather transcurrent region), north (Yakutat collision region), and Alaska (Alaska subduction region). This tectonic model is compared with a dynamic model that accounts for lithosphere strength contrasts and internal/boundary force balance. We argue that most of the Canada–Alaska Cordillera is an orogenic float where current tectonics are mainly limited to the upper crust, which is mechanically decoupled from the lower part of the lithosphere. Variations in deformation style and magnitude across the Cordillera are mostly controlled by the balance between plate boundary forces and topography-related gravitational forces. In particular, the strong compression and gravitational forces associated with the Yakutat collision zone are the primary driver of the complex tectonics from eastern Yukon to central Alaska, resulting in crustal extrusion, translation, and deformation across a $1500 \times 1000\text{-km}^2$ region. This tectonic–dynamic model can be used to provide quantitative constraints to seismic hazard models. We present a simple example of mapping $M_w = 7$ earthquake return periods throughout the Cordillera.

1. INTRODUCTION

The Canada–Alaska Cordillera is a broad plate boundary zone that has accommodated relative motion between the core of the North America plate and various oceanic plates

Active Tectonics and Seismic Potential of Alaska
Geophysical Monograph Series 179
Published in 2008 by the American Geophysical Union.
10.1029/179GM17

over more than 200 Ma. Detailed tectonic history of the Canadian and Alaskan Cordillera can be found in the works of *Gabrielse* [1992], *Monger and Price* [2002], *Plafker and Berg* [1994], and *Colpron et al.* [2007]. The Cordillera was formed mainly during the Mesozoic by the accretion of oceanic and island-arc terranes to the Paleozoic rifted margin of North America. Terrane accretion, northward translation, and deformation continue to the present. The large-scale tectonics of the Canada–Alaska Cordillera have been similar to

the present-day situation since about the mid-Cenozoic. The present Cordillera can be divided into four main tectonic provinces, from south to north (Plate 1): the Cascadia subduction zone, the Queen Charlotte–Fairweather transform region, the Yakutat collision zone, and the Alaska–Aleutian subduction zone. All four tectonic domains, including the main plate boundary faults, currently accommodate 40–60 mm/a of relative motion between the North America plate to the northeast and the Pacific and Juan de Fuca oceanic plates to the southwest [e.g., *DeMets et al.*, 1990].

In contrast with a standard “plate tectonics” model, where all the relative plate motion is accommodated along single major faults at the edge of non-deforming plates, the Canada–Alaska Cordillera represents a long-lived plate boundary zone [e.g., *Stein and Freymueller*, 2002; *Thatcher*, 2003]. Strain partitioning occurs at various levels across inboard faults and structures. For example, the south-central Alaska region is clearly recognized as an area of distributed deformation far within the Cordillera interior associated with the collision–subduction transition in the Gulf of Alaska [e.g., *Glen*, 2004; *Page et al.*, 1995; *Plafker et al.*, 1994]. Conversely, the central Cordillera is commonly, albeit falsely, viewed as a simple tectonic system where all relative motion occurs along the Queen Charlotte–Fairweather Fault.

In this chapter, we present an integrated set of seismic, geodetic, and geodynamic data that cover the Cordillera from southern British Columbia to central Alaska. These kinematic, tectonic, and dynamic markers are compared and combined to show that the Cordillera is a 400- to 1000-km-wide plate boundary zone. A small part (10–30%) of the relative plate motions is accommodated through distributed internal deformation of the weak Cordillera lithosphere; the Cordillera can be described as an orogenic float [e.g., *Oldow et al.*, 1990] with various levels of strain partitioning. Based on a comparison of the current tectonics, lithosphere strength contrasts, and internal and boundary force variations, we argue that the partitioning of deformation across the width of the Cordillera is mainly controlled by the balance between plate boundary forces and gravitational forces related to differential topography.

Our first-order tectonic–dynamic model provides a framework for more detailed studies of the tectonics in specific regions of the Cordillera. The model can also serve as a regional framework for seismic hazard assessment. The first-order geodynamics control the locations and return period statistics of earthquakes and can be used to define a large-scale earthquake hazard model.

2. CURRENT TECTONICS

Our model of present-day tectonics is primarily based on a combination of earthquake and geodetic data analysis. These

data sets and the derived crustal deformation information are presented separately before we discuss the combined model.

2.1. Earthquake Statistics and Seismic Strain

The distribution of seismicity provides a good illustration of the current deformation across the Cordillera. As shown in Plate 2, the density of earthquakes decreases eastward, from high concentrations along the western continental margin to low concentrations in the central, northern, and eastern regions. In contrast to the relatively uniform distribution on the western border, the earthquake density is highly variable in the Cordillera interior (e.g., northern British Columbia versus central Alaska). Earthquake focal mechanisms define the principal deformation regimes, which mostly vary between shortening and strike-slip [*Ristau et al.*, 2007]. In contrast with the western U.S. Cordillera, there is very little evidence of present-day extension in the Canada–Alaska sections (Plate 2). In most regions, earthquake mechanisms are compatible with the widespread NE–SW orientation of principal horizontal compression in the North America plate [e.g., *Zoback and Zoback*, 1991].

2.1.1. Method. Earthquake catalogs can also be used to derive quantitative estimates of crustal deformation. The method consists in summing the seismic moment contributions from individual earthquakes within a given seismic zone over a given period. The total moment can then be converted to rates of seismic moment release, seismic strain, and relative motion across the zone. Estimating crustal deformation from an earthquake catalog requires several general assumptions regarding the temporal and spatial patterns of seismic moment release. As a result, special care must be given to the uncertainties in the final results.

We use a method based on the integration of earthquake magnitude–frequency statistics, up to an estimated maximum magnitude, to derive moment rates and relative block motion rates [*Hyndman et al.*, 2003; *Mazzotti and Adams*, 2005]. The main advantage of this method is that it enables the statistics of small earthquakes to constrain the return period of the infrequent large events that account for most of the deformation. Thus, we can derive seismic deformation rates in regions where few or no large earthquakes have occurred in historical or instrumental times. The main assumptions are: (1) earthquake temporal distributions are stationary; (2) catalogs are complete for all magnitudes larger than 3.0–3.5, depending on the seismic zone; (3) all earthquakes within a given zone are representative of the same style of deformation and can thus be added in a simple scalar manner; and (4) the maximum earthquake magnitude in a zone can be estimated from local geologic data (maximum fault area) or by

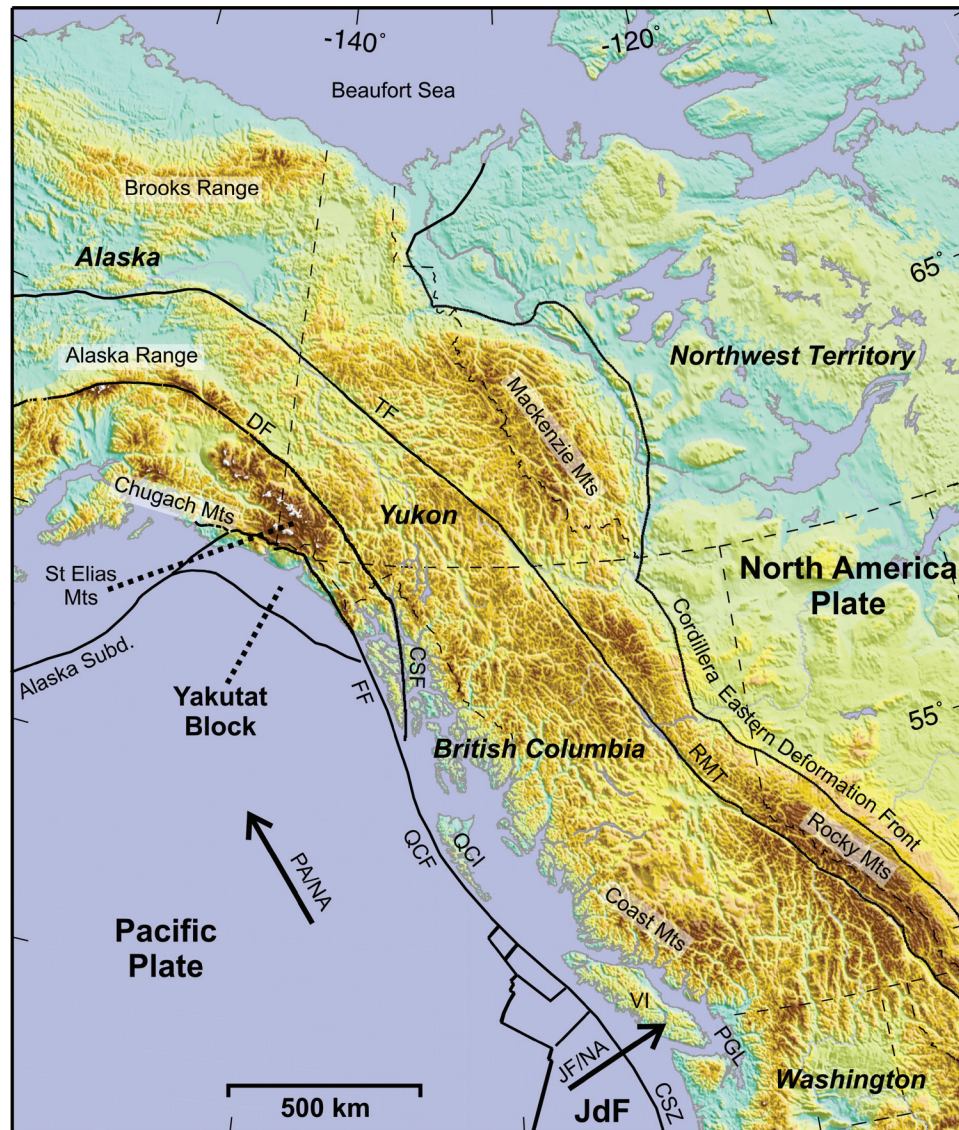


Plate 1. Topography and main tectonics. JdF, Juan de Fuca Plate; CSF, Chatham Strait Fault; CSZ, Cascadia subduction zone; DF, Denali Fault; FF, Fairweather Fault; PGL, Puget–Georgia Lowland; QCF and QCI, Queen Charlotte Fault and Islands; RMT, Rocky Mountain Trench; TF, Tintina Fault; VI, Vancouver Island.

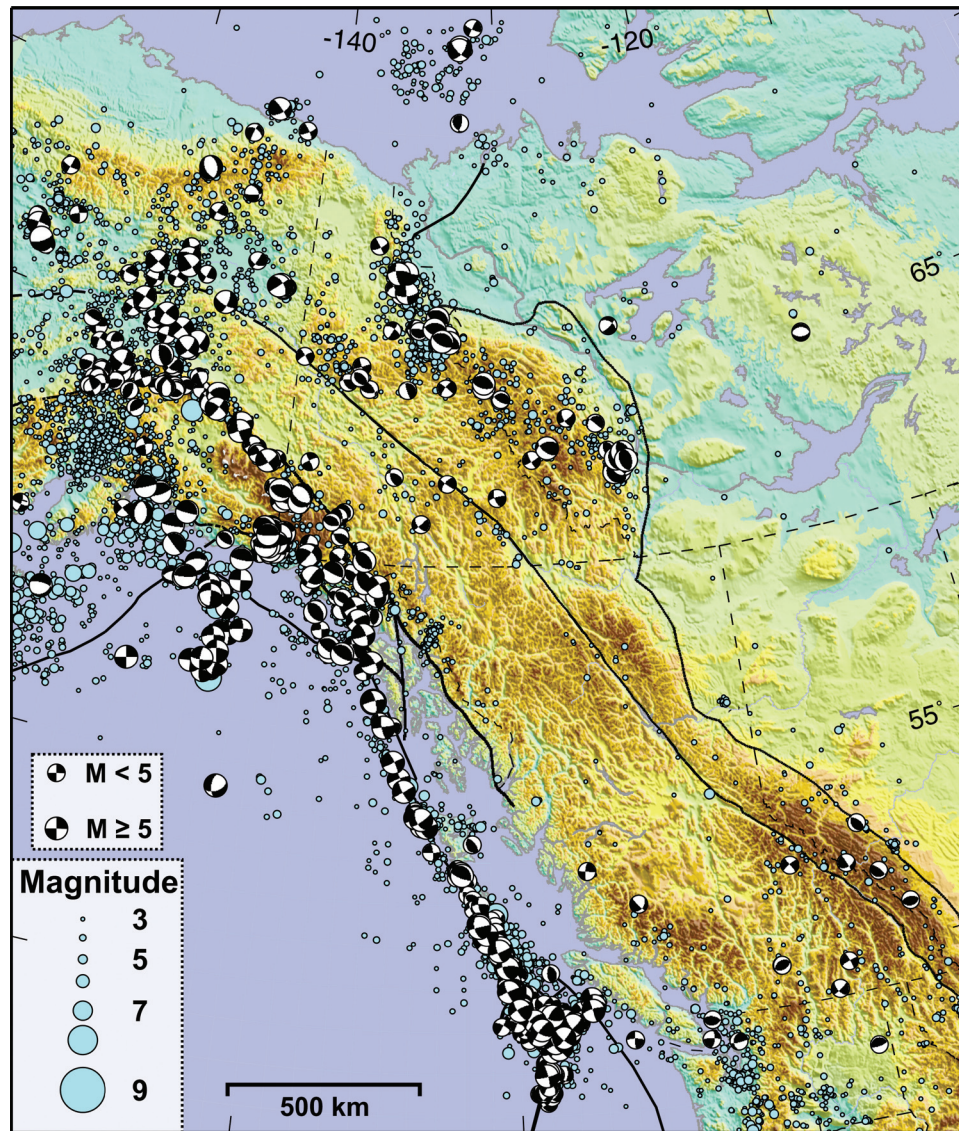


Plate 2. Earthquakes and focal mechanisms. Earthquakes of magnitude $M \geq 3$ since 1960 compiled from the Geological Survey of Canada, University of Alaska Fairbanks, and University of Washington catalogs. Focal mechanisms from the Harvard CMT catalog, the Geological Survey of Canada RMT catalog, and first-motion solutions.

comparison with other similar zones. Assumption 1 is only valid if we consider the seismicity at a scale large enough to avoid short-period and short-wavelength complexities. All these assumptions contribute levels of uncertainty that vary significantly with the level of knowledge of individual seismic zones.

We have previously applied the statistic integration method to different tectonic regions of the United States and Canada (Queen Charlotte Fault Zone, Puget–Georgia Lowland, St. Lawrence Valley, Yukon) and found that, to a first order, the estimated seismic deformation rates are in good agreement with geodetic and geologic rates [Hyndman and Weichert, 1983; Hyndman *et al.*, 2003; Mazzotti *et al.*, 2005; Leonard, 2006]. In the most recent studies, the estimation of uncertainties on the seismic deformation rates has been based on a statistical logic-tree approach, which allows including uncertainties on the parameters and models used in the calculations [Mazzotti and Adams, 2005]. The final uncertainties are usually fairly large (roughly a factor of 25–75%) and probably conservative. The rates presented here for the Yukon and Alaska regions are simplified from the more detailed results of Leonard [2006]. Rates in British Columbia are based on the earthquake catalog that was used to produce the 2005 National Seismic Hazard Maps of Canada [Adams and Halchuck, 2003].

2.1.2. Seismic deformation. The estimated seismic deformation rates for the Canada–Alaska Cordillera are shown in Figure 1, with the relative motion across the seismic zones based on focal mechanisms. Deformation is divided into four order-of-magnitude categories that can be distinguished

within the estimated uncertainties: <0.1, 0.1–1, 1–10, and 10–50 mm/a. Seismic slip rates on the three main plate boundary faults (Cascadia and Alaska subduction thrusts and Queen Charlotte–Fairweather transform) are significantly larger than elsewhere in the Cordillera. They range between 30 and 60 mm/a, in agreement with the relative plate motions, confirming that a large fraction of this relative motion is accommodated along the western margin. In most of the Cordillera, seismic deformation rates are very low (less than ~0.1 mm/a). Three regions have higher seismicity rates of 1–10 mm/a: the southern Canadian Cordillera forearc, the northern Canadian Cordillera Foreland belt, and central eastern Alaska. A few regions of small but resolvable rates (0.1–1 mm/a) also exist, mostly near or between more active zones (Figure 1).

The southern Canadian Cordillera marks a zone of transition from N–S compression and shortening in northern Washington and southernmost British Columbia to NE–SW compression and shortening in the Rocky Mountains of British Columbia [Plate 2, Ristau *et al.*, 2007]. Deformation rates drop by an order of magnitude between the two regions (Figure 1). In the rest of the British Columbia Cordillera, seismicity is very sparse and mostly associated with low (0.1–1 mm/a) right-lateral shear within ~200 km of the western margin.

North of the major seismicity gap in the central Cordillera, seismic deformation rates increase in the northern Cordillera [e.g., Cassidy *et al.*, 2005]. Most of the Yukon and eastern Alaska exhibit significant seismic strain, although some large gaps can be identified (Figure 1). Outside the plate boundary fault systems, the main regions of significant

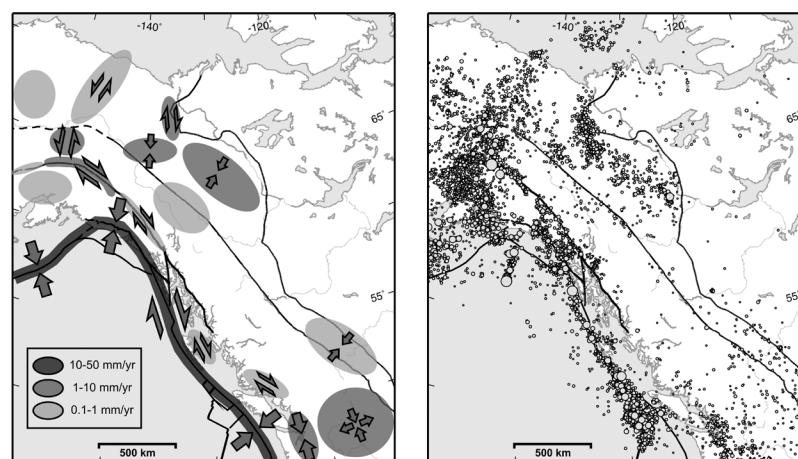


Figure 1. Seismic deformation rates. (left) Rates and style of crustal deformation derived from earthquake statistics integration and focal mechanisms (see text). Deformation rates expressed in terms of relative motion across seismic zones and divided into three categories: 0.1–1, 1–10, and 10–50 mm/a. (right) Earthquake epicenter map for reference (compare Plate 2).

seismic deformation (1–10 mm/a) are the Yukon–Northwest Territories Foreland Belt, including the Richardson Mountains strike-slip zone, and the region around and directly north of the central Alaska Range. We estimate that 10–30% of the relative Pacific–North America motion is accommodated across the large strike-slip and thrust fault systems in these areas. In contrast, slower seismic deformation (0.1–1 mm/a) is observed in the central and southern Yukon, northern Alaska, and southeastern Alaska.

2.2. Present Kinematics Defined by GPS

2.2.1. GPS data and transient corrections. The GPS has become the main tool for high-precision determination of crustal velocities in tectonic regions. Plate 3 shows a compilation of GPS horizontal velocities derived from continuous station and campaign-style measurements north of 46°N over the last decade. The map is based on a subset of, and additions to, previous regional studies in the southern, central, and northern parts of the Cordillera [Mazzotti *et al.*, 2003a, 2003b; Bustin, 2006; Leonard *et al.*, 2007]. Data from these studies as well as from new campaign sites are analyzed consistently and combined to provide the first coherent map of crustal deformation throughout the Canada–Alaska Cordillera (Plate 3). Details of the GPS processing are described by Mazzotti *et al.* [2003a] and Leonard *et al.* [2007]. The results are aligned to the International Terrestrial Reference Frame 2000 (ITRF2000) global reference frame [Altamimi *et al.*, 2002] by constraining the IGS core station Yellowknife (YELL) to its ITRF2000 position and velocity. A direct comparison with other GPS analyses in the ITRF2000 frame shows that our results, although aligned through only one station, are not affected by any systematic bias or distortion. Velocities are referenced to stable North America as defined by the ITRF2000/North America rotation vector [Altamimi *et al.*, 2002].

Our GPS velocity map can be used to help define the western edge of stable North America. As expected, all the sites located east of the Cordillera deformation front show very low horizontal velocities (<1 mm/a, Plate 3). However, one of the main questions of this study is the extent to which sites within the Cordillera can be currently attributed to stable North America, thus indicating no significant present deformation. To address this question, transient deformation recorded in the GPS data must be accounted for and corrected to derive an estimate of the long-term (geologic) tectonics. The transient signals related to earthquakes, slow-slip events, interseismic, and other nonpermanent deformation sources, and the associated corrections we consider are the following:

1. Cascadia subduction system: From about 46° to 50°N, GPS stations near the coast show a systematic eastward decrease of the velocities (Plate 3) that can be attributed to interseismic strain accumulation along the locked Cascadia subduction thrust [e.g., Miller *et al.*, 2001; Mazzotti *et al.*, 2003a]. Smaller transient deformation also occurs in the form of repeating slow-slip events along the deeper part of the subduction thrust [Dragert *et al.*, 2001]. Corrections of the interseismic locking and slow-slip effects are described in detail by Mazzotti *et al.* [2003a] and based on an elastic dislocation model of the subduction thrust [Wang *et al.*, 2003].
2. Queen Charlotte–Fairweather Fault system: Between about 50° and 59°N, the GPS velocities indicate right-lateral shear related to the transpressive Pacific–North America relative motion. Corrections of elastic strain associated with the interseismic locking of the Queen Charlotte and Fairweather Faults, as well as a potential underthrusting fault under the margin, are based on an elastic dislocation model tuned to the local variations in fault geometry and slip rates [Mazzotti *et al.*, 2003b; Bustin, 2006].
3. Yakutat–St. Elias region: GPS data in northwestern British Columbia, southwestern Yukon, and southeastern Alaska are affected by glacial isostatic adjustment from the post-Little Ice Age melting of glaciers in this area. Corrections for this transient signal are based on a viscoelastic model [Larsen *et al.*, 2005] and are described by Leonard *et al.* [2007]. These corrections reduce the amplitude of the northward motion in southwest Yukon–Alaska Panhandle by ~50% (Plate 3 versus Plate 4).
4. Alaska subduction system: Current deformation in the northwestern part of the Cordillera is influenced by the Alaska subduction zone. Interseismic locking and strain accumulation along the subduction thrust result in large margin-normal velocities that decrease landward (Plate 3). Significant postseismic relaxation following the 1964 great earthquake [e.g., Freymueller *et al.*, 2000; Zweck *et al.*, 2002] as well as a 2-year slow-slip event [Ohta *et al.*, 2006] result in trenchward motions at some of the forearc stations. We correct for the interseismic loading and postseismic effect by using the models of Sauber *et al.* [1997] and Zweck *et al.* [2002]. The effect of the slow-slip event is not accounted for (see discussion below).
5. Denali Fault system: The 2002 Denali earthquake had a very significant effect on GPS data in most of Alaska and Yukon [e.g., Hreinsdóttir *et al.*, 2006; Leonard *et al.*, 2007]. Both coseismic and postseismic transients are corrected for at far-field sites (more than 100 km

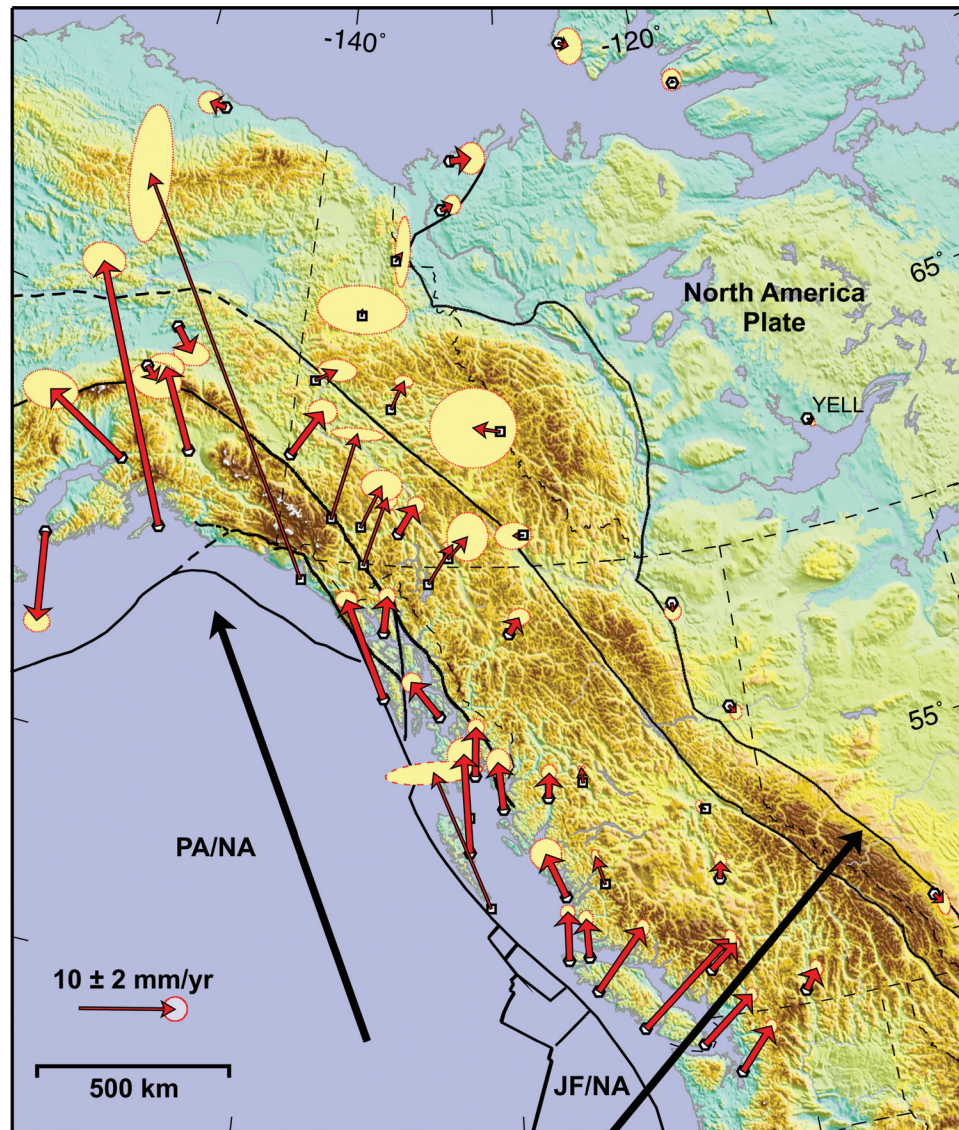


Plate 3. Present-day GPS kinematics. Horizontal GPS velocities with respect to North America. Yellow ellipses are 95% confidence regions. Continuous and campaign GPS velocities shown by thick and thin arrows, respectively. Thick black arrows show Pacific–North America [Altamimi *et al.*, 2002] and Juan de Fuca–North America [Mazzotti *et al.*, 2003a] relative motions.

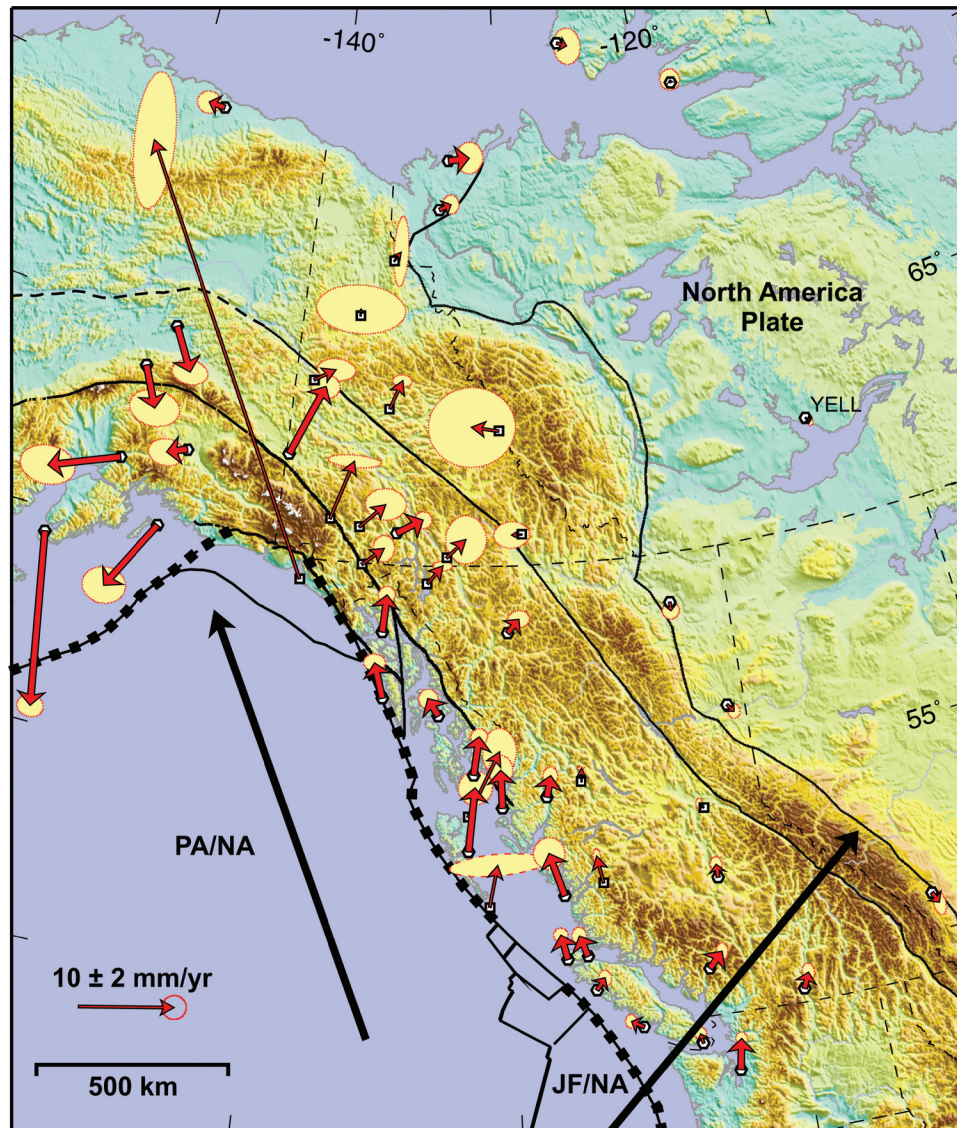


Plate 4. Residual GPS velocities. Horizontal residual GPS velocities, with respect to North America, after correction for main interseismic and glacial isostatic transients (see text). Locked plate boundary faults are shown by thick dashed lines. GPS symbols and uncertainties as in Plate 3. Uncertainties do not account for transient correction effects.

away from the fault) using elastic and viscoelastic model predictions [Hreinsdóttir *et al.*, 2006; Freed *et al.*, 2006]. For near-field sites, these effects are avoided by limiting the data to pre-earthquake time spans.

2.2.2. Long-term kinematics from GPS. Plate 4 shows GPS residual velocities after corrections for the various transient deformations described above. Uncertainties from these corrections are difficult to assess, but the residual velocities are probably associated with uncertainties ~ 1 mm/a larger than the original velocities. This extra uncertainty level is omitted in Plate 4 for clarity.

In the southern Cordillera, GPS rates of 5–10 mm/a in central Washington represent a permanent northward translation and deformation that extends to southernmost Vancouver Island [McCaffrey *et al.*, 2000, 2006; Mazzotti *et al.*, 2002]. A small strain transfer within the southern British Columbia Cordillera is also possible. Most sites show a small N to NE velocity (1–3 mm/a, Plate 4) that could be attributed to unmodeled subduction loading, postseismic relaxation from the 1700 great earthquake [Wang *et al.*, 2003], permanent motion and strain across the Cordillera [Mazzotti *et al.*, 2003a; McCaffrey *et al.*, 2006], or any combination of these.

The change of regime between Juan de Fuca subduction and Pacific–North America transpressive tectonics appears to occur in northern Vancouver Island [Mazzotti *et al.*, 2003a]. Farther north in the Queen Charlotte Islands and Alaska Panhandle, the residual GPS data indicate a permanent right-lateral shear of the margin or coastal sliver motion [Mazzotti *et al.*, 2003b]. The residual velocities exhibit a significant northward motion of ~ 5 mm/a that propagates landward into the Coast Mountains and decreases abruptly to zero in the central part of the Cordillera (Plate 4). However, this residual field is particularly sensitive to the details of the interseismic loading model and more complex viscoelastic models might account for most of the apparent residual deformation.

Farther north, the coastal shear/sliver motion appears to merge with pronounced deformation related to the ongoing collision of the Yakutat block. Southwest of the main collision front (Chugach–St. Elias Mountains), the residual velocities are similar to the Pacific–North America velocity (~ 45 mm/a at Yakutat versus ~ 55 mm/a), whereas they decrease to ~ 5 mm/a directly on the northeast side [e.g., Fletcher and Freymueller, 2003]. This very high strain rate is in agreement with the active seismicity showing that most of the Yakutat–North America relative motion is accommodated within a 100- to 200-km-wide deformation zone [Leonard *et al.*, 2007]. The ~ 5 mm/a NE to NNE residual motion confirms that $\sim 10\%$ of the Yakutat–North America convergence

is transmitted through the collision zone and transferred to the central part of the northern Cordillera, possibly as far inland as the eastern Cordillera front [Mazzotti and Hyndman, 2002; Hyndman *et al.*, 2005b; Leonard *et al.*, 2007].

The residual GPS velocities in the Alaska forearc are subject to corrections with large uncertainties and should be interpreted with caution. In particular, the 1998–2001 slow-slip event may bias our residual velocities by as much as 5–10 mm/a trenchward [Ohta *et al.*, 2006], although we do not see indications for significant transients associated with this event in our post-1999 time series. Residual velocities appear to indicate a westward to southwestward motion of the Alaska forearc at 10–15 mm/a (Plate 4), consistent with the proposed counterclockwise rotation of a forearc block and extrusion away from the Yakutat collision zone [e.g., Fletcher, 2002; Redfield *et al.*, 2006]. Farther inland, the sites on the south and north sides of the Alaska Range exhibit a combination of shortening and right-lateral shear tectonics in relation to the Denali Fault and the complex deformation zone between the Denali and Tintina Faults [e.g., Page *et al.*, 1995; Leonard *et al.*, 2007].

2.3. Cordillera Tectonic Model

The seismicity and GPS data can be combined to produce a first-order model of present-day tectonics in the Canada–Alaska Cordillera. Plate 5 shows our schematic tectonic map with the general styles and rates of deformation that define the main tectonic zones of the Cordillera. As discussed in the previous sections, 70–90% of the relative motion between the North America plate and the Pacific–Juan de Fuca plates is accommodated within a narrow zone along the western margin of the Cordillera. In most regions, this zone is limited to the major plate boundary faults (subduction or transform). In the case of the Yakutat collision system, the main deformation zone extends over ~ 100 km across the Chugach–St. Elias shortening region (Plate 5).

The remaining 10–30 % of the relative plate motion is distributed over regions of varying spatial extents. In the Yukon–Alaska area, strain partitioning occurs over the whole width of the Cordillera with active tectonic zones as far as 800–1000 km from the main plate boundary. This pattern also applies, although to a smaller degree, to the southern Cordillera where $\sim 5\%$ of the Juan de Fuca–North America convergence may be accommodated across the Cordillera and in the Foreland Belt. In contrast, the central Cordillera shows a more focused strain distribution zone. Most of the Pacific–North America transform motion is accommodated on the Queen Charlotte Fault, but the remaining $\sim 10\%$ may be taken up by right-lateral shear over a 300- to 400-km-wide system that extends into the Coast Mountains. Based on the

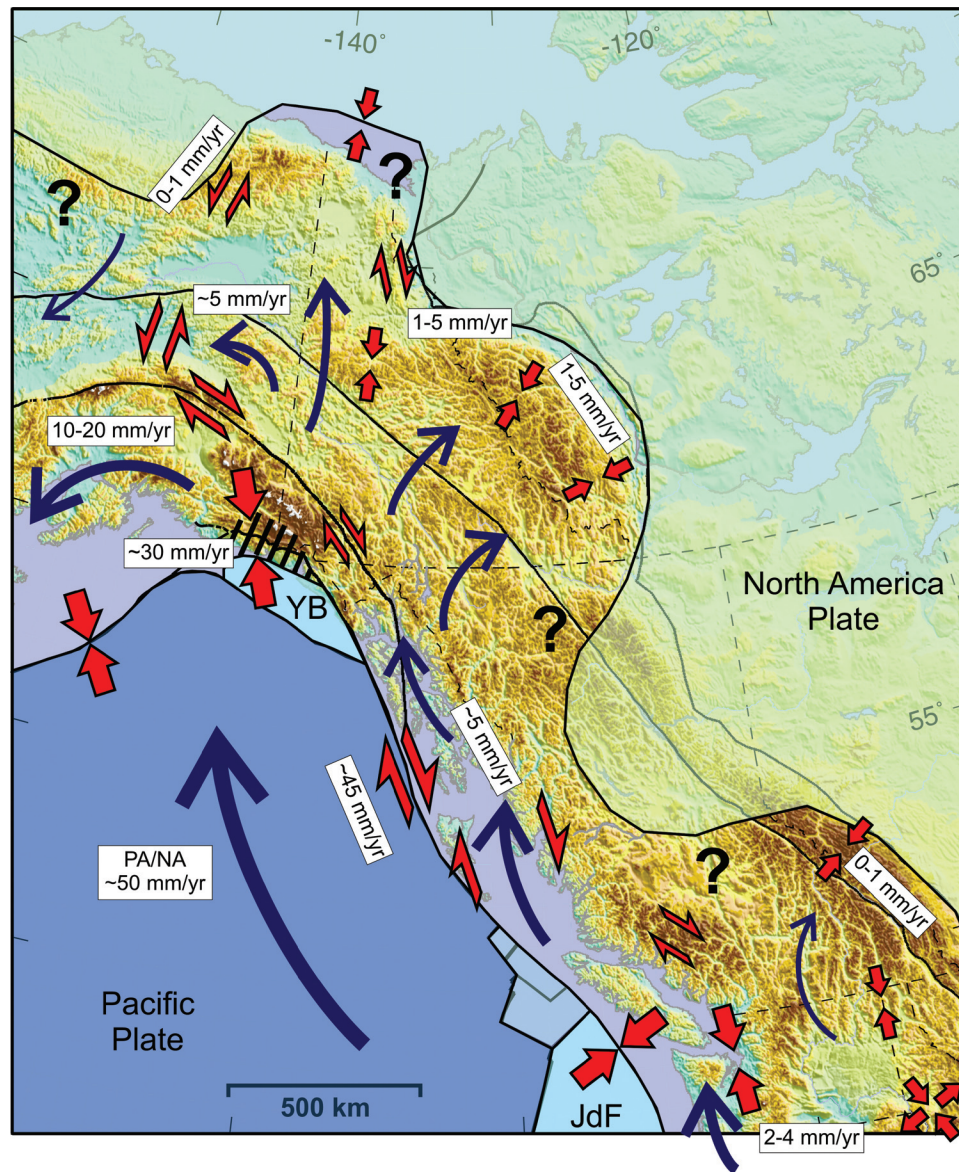


Plate 5. Active tectonics of the Cordillera. Tectonic model derived from earthquake statistics, focal mechanisms, and GPS data. Curved blue arrows show schematic motions of Pacific Plate (blue shade) and Cordillera internal blocks and deforming regions with respect to North America plate (green shade). Converging and shear red arrows indicate areas of shortening and strike-slip deformation, respectively. Dashed area marks main Yakutat collision zone. Extent of currently stable North America in central British Columbia, northern Yukon, and northwestern Alaska unclear. JdF, Juan de Fuca Plate; YB, Yakutat Block.

GPS data, a small component of margin-normal shortening also appears to be distributed within the Queen Charlotte–southern Panhandle deformation region.

The transitions between these large-scale tectonic domains are not clear. In southern British Columbia, the switch from subduction to strike-slip regimes appears to occur along the projection of the Juan de Fuca–Explorer slab northern boundary. In northern Vancouver Island, numerous geologic and geophysical evidences point to a change in the tectonic regime and the end of the subduction system [e.g., *Lewis et al.*, 1997; *Cassidy et al.*, 1998]. However, the small number of earthquakes contrasts with the left-lateral shear and extension suggested by the GPS data (Plates 2 and 4). Further inland, the transition may occur in the Coast Mountains, possibly associated with a small concentration of (strike-slip) earthquakes.

In northern British Columbia and southeastern Alaska, the transition from right-lateral shear to the Yakutat collision system appears to be on a series of faults and deformation zones, possibly involving the whole northwestern British Columbia region. GPS stations about 300–500 km to the southeast of the main collision zone show a small (2–5 mm/a) northeast motion that is likely related to the influence of the collision (Plate 4). The impact of the Yakutat collision is also likely responsible for the wide transition region with the Alaska subduction system to the west. Right-lateral strike slip on the Denali Fault is associated with counterclockwise rotation and westward extrusion of the Alaska forearc block in response to the collision [e.g., *Redfield and Fitzgerald*, 1993]. The relation between the Yakutat collision and the details of the far-field tectonics in the Dawson region, Richardson and Mackenzie Mountains, and northeastern Alaska is less obvious.

3. DYNAMICS OF THE CORDILLERA

In contrast to the western United States, the relation between tectonics and dynamics has been little explored in western Canada and Alaska. The balance of driving and resisting forces in the western U.S. Cordillera has been addressed in dozens of publications. It is generally agreed that the forces controlling the tectonics of the western United States are a combination of dextral shear traction along the California margin and gravitational forces in the central and eastern highlands [e.g., *Flesch et al.*, 2000; *Humphreys and Coblenz*, 2007]. Our tectonic model shows that the Canada–Alaska Cordillera can be similarly viewed as a large-scale plate boundary zone where the far-field relative plate motion is partitioned and distributed across various structures. The distinction among the four main tectonic domains discussed above provides an opportunity to address the balance

of lithosphere strength, driving, and resisting forces controlling the current tectonics.

3.1. Lithospheric Strength and Orogenic Float

Hyndman et al. [2005a] argue that backarc regions worldwide have hot, thin, and weak lithospheres that form tectonically active mobile belts (plate boundary zones) along colder, thicker, and stronger stable continental plates. The Canada–Alaska Cordillera may represent an archetype of hot backarc mobile belts such as the Andean Cordillera or Southeast Asia.

Upper mantle shear wave velocity (V_s) is directly related to temperature and is a good proxy for lithospheric strength. Plate 6 shows V_s anomalies at 100-km depth, with a strongly bimodal distribution of low V_s under the Cordillera and high V_s under the stable continent [*Van der Lee and Frederiksen*, 2005]. Second-order variations exist within these regions, but they are small compared with the first-order contrast. As discussed by *Currie and Hyndman* [2006], low V_s in the Canada–Alaska Cordillera is associated with a hot geotherm, temperatures of the order of 700°–900°C at the Moho, and a thermal lithosphere thickness of ~60 km. In contrast, high V_s in the stable (Paleozoic and older) continent is associated with a cold geotherm, temperatures of 400°–600°C at the Moho, and a lithosphere thickness of 150 km or more. In oceanic plates, the geotherm and lithosphere thickness are direct functions of the plate age. The Juan de Fuca and Pacific plates offshore the Cordillera are young (0–40 Ma) with lithosphere thicknesses of 20–60 km. However, the thin oceanic crust (7 km) results in low temperatures and strong brittle behavior in the uppermost mantle. Therefore, the oceanic lithosphere as a whole is quite strong, except very near the triple junction off northern Vancouver Island.

The important implication of these temperature differences for large-scale tectonics is the resulting contrast in crustal and upper mantle strength. Total lithosphere strength can be estimated using yield stress depth profiles and integrating the differential stress over the lithosphere thickness [e.g., *Kohlstedt et al.*, 1995; *Ranalli*, 1995]. Although the details of this method, especially the predicted strength contrasts between the lower crust and upper mantle, remain debated [e.g., *Jackson*, 2002], the yield stress envelope provides a good first-order estimate of the integrated lithosphere strength under a range of temperature conditions. Because of the very high temperatures in the Cordillera lower crust and upper mantle, most of the lithosphere strength is estimated to reside in the upper crust and the integrated strength is only 1×10^{12} to 3×10^{12} N/m. In contrast, the cold temperatures in the stable continent allow for significant differential stress in the lower crust and upper mantle, with an integrated strength

of more than 50×10^{12} N/m, at least 10 times larger than in the Cordillera [e.g., *Hyndman et al.*, 2005a]. Similarly, the integrated strength of oceanic lithosphere (mainly between 0 and 30 km) is much higher than that of the Cordillera, except near the hot triple junction off northern Vancouver Island.

Another important consequence of the hot geotherm in the Cordillera is that both the lower crust and the upper mantle mostly deform by viscous creep under very low differential stress. In contrast, the upper crust remains for the most part within the brittle deformation regime and sustains much higher differential stress [e.g., *Townend and Zoback*, 2000]. Thus, yield stress curves for the Cordillera show a high-stress brittle upper crust over a low-stress viscous lower crust and upper mantle. This situation leads to the concept of a thin upper-crust orogenic float, divided into semirigid blocks bounded by active faults and mechanically decoupled from the lower crust and upper mantle [e.g., *Oldow et al.*, 1990]. This concept was proposed by *Mazzotti and Hyndman* [2002] to explain the far-field strain transfer from the Yakutat collision across the northern Cordillera.

This orogenic float model can be extended to the Canada–Alaska Cordillera as a whole. Based on seismic and heat flow data (Plate 6), the average temperature conditions in the lower crust are inferred to be fairly constant over the whole region at 700°–900°C. Seismic velocity and xenolith data also argue for a high water content in the upper mantle and probably throughout the lithosphere (see discussion by *Hyndman et al.* [2005a]). These conditions are sufficient for a general mechanical decoupling of the upper crust over the lower crust and upper mantle. In specific regions, such as the Cascadia and Alaska forearcs or the eastern Foreland Belts, mechanical coupling throughout the lithosphere probably occurs because of colder geotherm conditions.

3.2. Force Balance

If the entire Canada–Alaska Cordillera is indeed a low-strength orogenic float between three strong plates, then the temporal and spatial variability in large-scale tectonics must result from variations in the balance between driving and resisting forces. By comparison, the variations in tectonic style in the western United States result mainly from the competition between boundary forces along the western margin and high gravitational potential energy in the Basin and Range and Rocky Mountains [e.g., *Jones et al.*, 1996; *Flesch et al.*, 2000].

Humphreys and Coblenz [2007] provide an extensive quantitative model of forces affecting the North America plate. In order of decreasing importance, the three main categories are plate boundary forces, gravitational potential

energy, and basal friction/drag. In particular, their model requires significant shear traction along the San Andreas system ($\sim 1.5 \times 10^{12}$ N/m), slab pull along the southern Cascadia subduction zone ($\sim 3 \times 10^{12}$ N/m), and gravitational collapse of the U.S. Cordillera (1×10^{12} to 3×10^{12} N/m) to explain the stress indicators in the western United States. These force amplitudes, typical of tectonic force estimates [1×10^{12} to 5×10^{12} N/m, e.g., *Whittaker et al.*, 1992], easily account for the contrast in deformation between mobile belts and stable continental/oceanic plates. Because of their high geotherms, backarc mobile belts are weak enough to deform at fast tectonic strain rates (10^{-14} to 10^{-16} s $^{-1}$), whereas cold intraplate regions are much stronger and can deform only at much slower rates ($\leq 10^{-18}$ s $^{-1}$, e.g., *Zoback et al.*, 2002].

The North America force balance model of *Humphreys and Coblenz* [2007] also provides a good reference for explaining the current tectonics of the Canada–Alaska Cordillera. Our conceptual dynamic and tectonic model is shown in Plate 7. The Cordillera is under a general NE–SW to N–S compression maintained by the balance between gravitational potential energy of the mid-Atlantic ridge, transmitted throughout eastern and central North America lithosphere [*Zoback*, 1992], and margin-normal compression along the north Cascadia, Queen Charlotte–Fairweather, Yakutat, and eastern Alaska boundaries. However, this first-order picture does not account for the variations in tectonic style between the four main domains. We argue that these variations are controlled by the more local balance between boundary and gravitational topography-related forces.

Gravitational forces (F_G) are commonly viewed as the main source of tensional stress in the U.S. Cordillera. There, F_G estimates vary between 0.5×10^{12} and 3×10^{12} N/m, depending mostly on elevation, crustal thickness, and buoyancy of the mantle [*Jones et al.*, 1996]. We estimate the F_G variations in the Canada–Alaska Cordillera based on average cross-section profiles in the four main tectonic domains (south, central, north, and Alaska). Details of the calculations are described in Appendix A and the results are shown in Figure A1. As expected, positive (tensile) F_G values (0×10^{12} to 2×10^{12} N/m) are limited to high elevations in the Coast Mountains, central plateau, and the Foreland Belt. Variations in F_G between these regions can reach $\sim 100\%$ in relation with changes in crustal thickness and lithosphere temperature/density. Uncertainties on the F_G values vary significantly, mostly because of poor data coverage in some of the remote regions of the Cordillera such as the St. Elias Mountains (compare Appendix A). The Alaska Foreland Belt also appears to be in a more complex state of isostasy and possibly compressive F_G , in response to the relatively low elevation and thick crust beneath the Brooks Range.

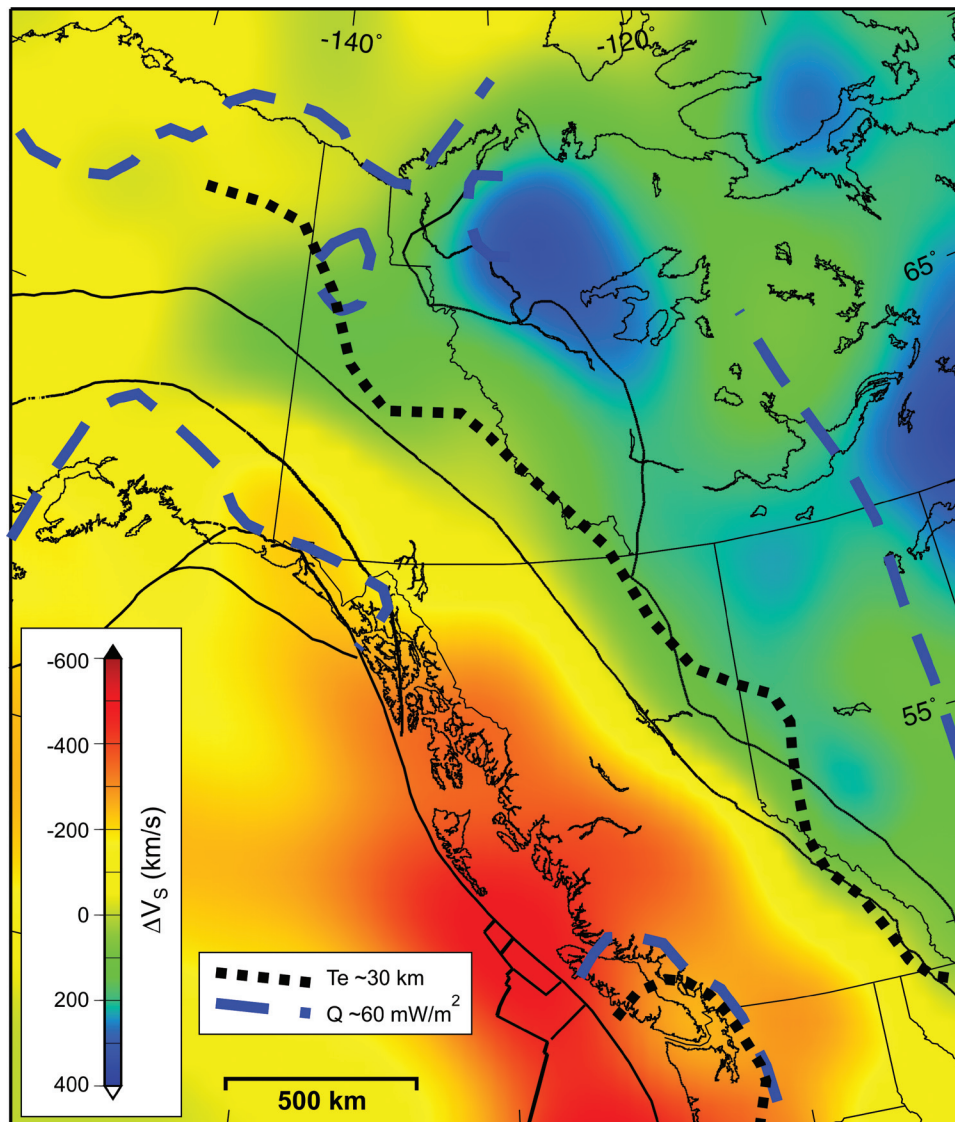


Plate 6. Mantle seismic velocity and lithosphere strength. Colored map shows mantle shear-wave velocity at 100 km depth [Van der Lee and Frederiksen, 2005]. Dashed black and blue lines show 30-km and 60-mW/m² transitions in effective elastic thickness [Flück et al., 2003] and surface heat flow [Lewis et al., 2003; Blackwell and Richards, 2004].

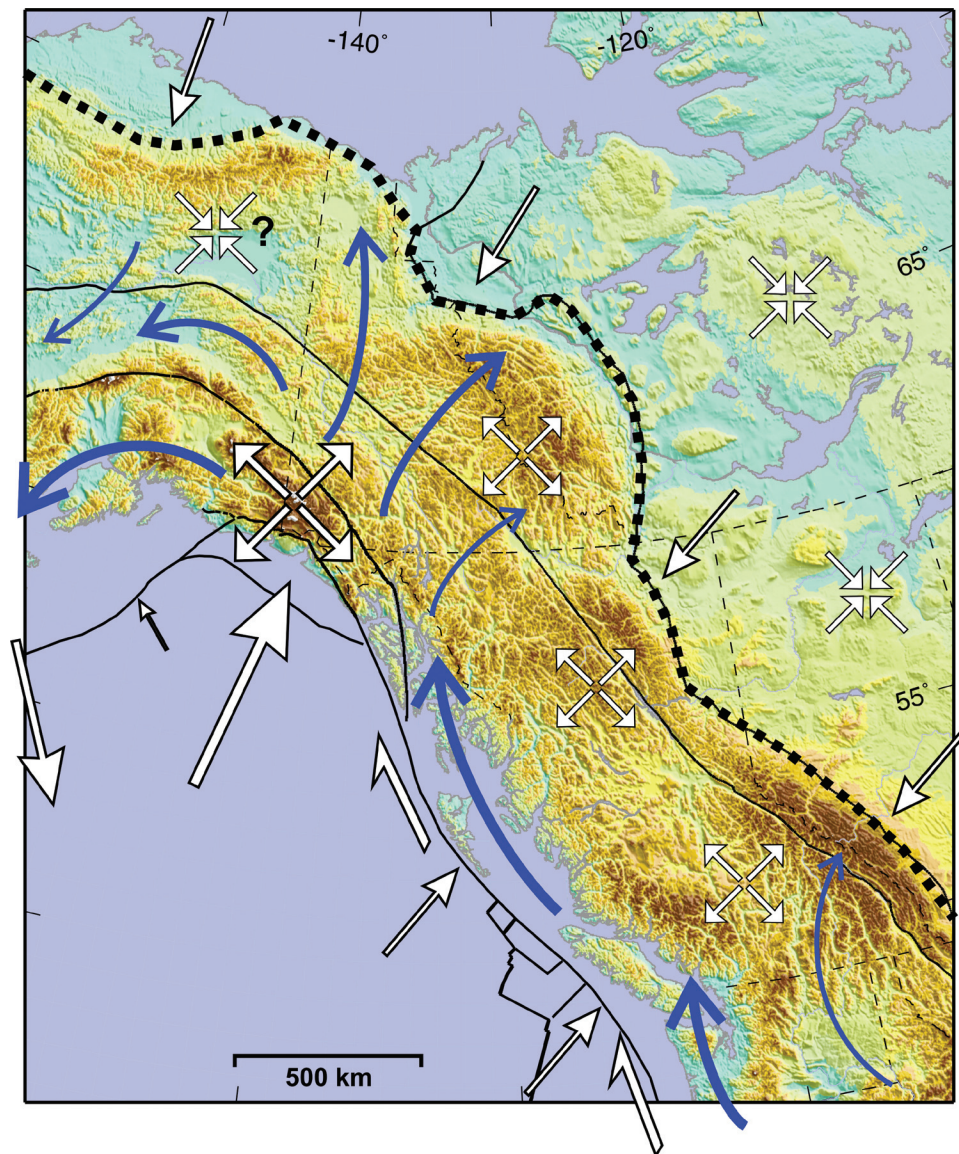


Plate 7. Dynamics of the Cordillera. Curved blue arrows show schematic motions of Cordillera internal blocks or deformation regions with respect to North America plate (Plate 5). White arrows indicate style and relative magnitude of boundary forces [Humphreys and Coblenz, 2007] and gravitational forces (Appendix A) acting on Cordillera orogenic float. Diverging and converging sets of arrows show tensile and compressive gravitational forces, respectively. Slab pull arrow of the central Alaska subduction zone displaced eastward.

Tensile F_G values in Canada are on average slightly lower than those for the Basin and Range regions, but they remain within the range of force amplitudes that could drive extension and collapse of the Cordillera topography (as occurred in southwestern British Columbia in the Eocene). Thus, the principal difference, and main tectonic control, between the U.S. and Canada–Alaska Cordilleras are the boundary forces. As pointed out by *Humphreys and Coblenz* [2007], the collapse and NW–SE extension of the Basin and Range province are only possible because of the strong slab pull of the south Cascadia subduction: the trench rollback promotes tensile stress in the upper plate and creates a “tectonic open end” along the subduction front. This is highlighted by the concentration of tension axes and material flow directions toward the Oregon coast. In contrast, the northern Cascadia region is characterized by margin-parallel compression and material flow, pointing toward a more compressive subduction zone. Thus, the lack of topography-driven extension in the Canadian Cordillera is related to the lack of “tectonic open end” that would allow outward flow of the stretched lithosphere [e.g., *Rey et al.*, 2001].

3.2.1. Northern Cordillera and impact of the Yakutat collision. The main exception to the generally compressive boundary-force state is the central Alaska subduction system, which is associated with significant slab pull/trench rollback [$\sim 3 \times 10^{12}$ N/m, *Humphreys and Coblenz*, 2007]. This provides the “tectonic open end” that allows southwestward extrusion of material away from the Yakutat collision zone (Plate 7). In this model, the current southwestward strike-slip tectonics of central and eastern Alaska are mainly driven by the high boundary compression and tensile F_G around the Yakutat collision zone but are permitted by the central Alaska subduction “open end.” The model is similar to other collision/extrusion systems where subduction zones provide the escape zone for outward material flow (e.g., Turkey–Greece or India–Southeast Asia).

To the east, the impact of high compression and F_G in the Yakutat collision appears to be diverted northeastward toward the Mackenzie Mountains and, possibly, the Richardson–Beaufort Sea area (Plate 7). *Mazzotti and Hyndman* [2002] argue that the collision system is the main driver for the high seismicity in the eastern Foreland Belt region. They also note that such a stress and strain transfer can only occur if (1) the upper crust is mechanically decoupled from the lower lithosphere (orogenic float concept) and (2) the Foreland Belt is characterized by a low strength, compared with the “typical” Cordillera strength. In this model, the Foreland Belt plays the role of the “tectonic open end,” although arguably not as efficiently as a subduction zone. Mechanisms for weak foreland belts have been much

discussed and probably are related to high pore-fluid pressure in very low-angle thrust sheets [e.g., *Cook et al.*, 1991].

3.2.2. Central–southern Cordillera dextral shear. The North America model of *Humphreys and Coblenz* [2007] suggests that a significant dextral shear traction (1×10^{12} to 3×10^{12} N/m) is applied along the entire western U.S. and Canada margin from the Pacific–North America transform and the oblique Juan de Fuca–North America subduction. This dextral shear results in the margin-parallel (roughly northward) motion of the whole western North America forearc or paleo-forearc region (e.g., Sierra Nevada block in California).

In the southern Cordillera (southern British Columbia–Washington), the clockwise rotation of the Oregon block along the Cascadia margin results in mostly northward motion and N–S shortening in the forearc [e.g., *Wells et al.*, 1998; *Mazzotti et al.*, 2002]. The nearly rigid rotation of the Oregon block appears to extend inland east of the Cascade volcanic arc and affect eastern Washington [*McCaffrey et al.*, 2006]. To a first order, this tectonic pattern can be explained by (1) Basin and Range F_G -driven northwestward flow, (2) Cascadia oblique-subduction dextral shear, and (3) margin-normal compression at the northern end of the Cascadia subduction zone preventing outward extension and flow of the Cordillera (Plate 7). A small part of the forearc and backarc northward motion may be transferred to the southern British Columbia Cordillera, resulting in the clockwise rotation of maximum horizontal compressive stress [Plate 2, *Ristau et al.*, 2007] and small shortening rates in the Foreland Belt (Figure 1).

Further north in the central Cordillera (50–59°N), the tectonic situation appears simpler. Dextral shear along the Pacific–North America boundary drives the margin-parallel motion of the Queen Charlotte–Panhandle area (Plates 4 and 7). This motion may also be facilitated by the inferred incipient subduction occurring at the southern end of the Queen Charlotte Fault system [e.g., *Hyndman and Hamilton*, 1993; *Smith et al.*, 2003]. Whether this motion occurs as distributed shear or a rigid block rotation is unclear. The Queen Charlotte–Alaska Panhandle area is the paleo-forearc of the early Cenozoic Resurrection plate subduction system [*Haeussler et al.*, 2003] and as such may have been cool. However, the post-Eocene ridge subduction, slab window, and subsequent extension have resulted in a high geotherm and thin crust in most of the Queen Charlotte region that may allow distributed shear in the weak lithosphere of that area.

At the northern end of this system, the northward transcurrent motion of the margin along the Queen Charlotte–Fairweather Fault joins with the Yakutat collision–northern Cordillera tectonic domain. The details of the connection are

not clear; seismicity and GPS data do not provide any evidence for strain transfer along the Chatham Strait and southern Denali Faults. The paleo-forearc motion appears to be partly deflected inland (northeast), away from the Yakutat collision and high F_G region (Plates 4 and 7).

4. IMPLICATIONS FOR SEISMIC HAZARD MODELS

The tectonic model presented in this study can be used to define a first-order background seismic hazard model for the Canada–Alaska Cordillera. The predicted crustal strain rates can be converted to rates of seismic moment release and earthquake return periods with some assumption on the form of the earthquake statistics, seismic volume (especially thickness), and local maximum magnitude. The inclusion of bulk strain rates from GPS or geologic studies provides additional constraints to seismic hazard models that are independent of instrumental and historical local earthquake catalogs. The method for earthquake hazard estimates is similar to that used to derive deformation rates from earthquake statistics (Section 2.1), except applied in reverse. For example, *Mazzotti et al.* [2005] used GPS-derived strain rates to estimate earthquake statistics (b and a values or maximum magnitude) along the St. Lawrence Valley, eastern Canada. The U.S. Geological Survey used a similar technique to include GPS-derived strain rates in their calculation of earthquake statistics and seismic hazard (i.e., ground shaking probabilities) in the Pacific Northwest [*Frankel et al.*, 2002].

Estimation of a seismic hazard model is beyond the scope of this chapter but could easily be done based on the deformation rates derived or discussed in our study. As an illustration we present a simple first-order estimate of seismic hazard in the form of return period of characteristic earthquakes of magnitude $M_w = 7$. We assume that (1) a $M_w = 7$ earthquake

is equivalent to ~ 1 m of slip on a 750 km^2 fault [*Wells and Coppersmith*, 1994]; (2) a seismic thickness of 15 km is a reasonable average for most of the Cordillera, where the seismic thickness controlled by the local geotherm varies between 10 and 30 km [*Mazzotti and Hyndman*, 2002]; (3) the relative motion measured across a given seismotectonic zone is uniformly distributed within this zone; (4) the length of a seismotectonic zone is defined along the strike of its primary fault-style (i.e., equivalent dip-slip or strike-slip through the entire zone); (5) crustal deformation is fully accommodated in earthquake strain release.

Based on these assumptions, a relative motion of 1 mm/a across a zone with an along-strike length of 100 km corresponds to a return period of 500 years for a characteristic $M_w = 7$ earthquake. Estimated return periods for the Cordillera seismotectonic zones are shown in Table 1 and Figure 2.

This simple approach obviously has some limitations. All five assumptions are associated with a significant level of uncertainty that propagates, for most parts linearly, to the estimated return periods. For example, assuming a seismic thickness of 15 km instead of an actual 30-km value results in a return period too small by a factor of 2. Since earthquake catalog statistics and focal mechanisms were used in the construction of our tectonic model, the derived earthquake return period map is not entirely independent of seismicity observations and interpretations. In several regions, the map reflects the actual earthquake catalog (e.g., Mackenzie Mountains) but with a tectonic interpretation added. In other areas, such as the Queen Charlotte–Alaska Panhandle margin, the map is mostly based on GPS data, and the predicted rate of $M = 7$ earthquakes is not reflected in the instrumental seismicity.

Finally, the most problematic limitation lies in our assumption that deformation is fully seismic within a given zone. The estimated return periods are clearly a minimum

Table 1. Relative Motions and Earthquake Return Periods^a

Zone	v , mm/a	L , km	T , $M = 7$
Puget–Georgia Lowland	2–4	150	125
South Rocky Mts.	0–2	500	500
South-central British Columbia	0–1	300	900
South Coast Mts.	0–2	300	850
Queen Charlotte margin	3–10	800	15
Mackenzie Mts.	1–5	500	60
Richardson Mts.	1–5	300	100
Brooks Range	0–1	500	550
Central Alaska	2–10	200	75
Central Denali Fault	5–10	500	15
Yakutat Collision	15–30	200	20
Eastern Denali Fault	1–5	400	75
Central Yukon	0–1	500	550

^a v , relative block motion; L , length of seismic zone; T , earthquake return period.

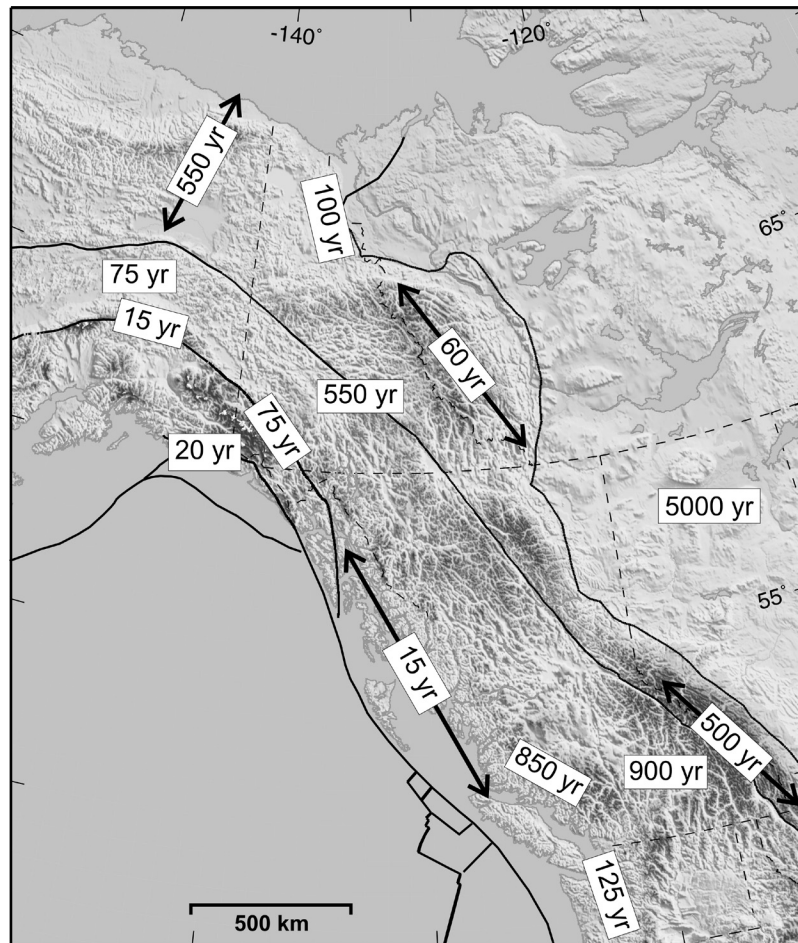


Figure 2. Earthquake return period and seismic hazard. First-order seismic hazard derived from active tectonic model (Plate 5) expressed in terms of return period of characteristic earthquakes of magnitude $M_w = 7$. Length of long seismotectonic zones shown by large arrows.

bound and may in fact be unrealistic in areas where a significant part of the deformation is aseismic. The Queen Charlotte margin, inland from the main Queen Charlotte Fault, provides a good example of this potential problem. Based on our model, we estimate a return period $T = 15$ a in this 800-km-long zone, in contrast to the actual earthquake catalog that shows no event larger than $M_w = 6.5$ in the last 100 years. This discrepancy is partly related to the sparse coverage of GPS sites that limits our tectonic model to a rough large-scale interpretation. However, the possibility that ~ 5 mm/a of dextral shear are accommodated within this zone (Plate 4) points to a fundamental issue in our understanding of how and where strain is accommodated in this area (e.g., seismic or aseismic, focused strike-slip faulting or distributed shear).

5. CONCLUSION

Compared with the western United States, active tectonic studies in the Canada–Alaska part of the North America Cordillera are relatively sparse and tend to focus on a few specific features such as the Cascadia and Alaska subduction zones or the Yakutat collision zone. The paucity of studies is partly because of the relatively low deformation rates and limited accessibility. These factors have led to a general view of the northern half of the North America Cordillera as being mostly tectonically inactive inboard of the main plate boundary fault systems [e.g., World Strain Map project, *Kreemer et al.*, 2003].

Our first-order quantitative tectonic model of the Canada–Alaska Cordillera, based on the integration of seismicity

and GPS data, shows that the relative plate motion is in fact distributed throughout the Cordillera over distances varying between 400 and 1000 km. Most of the relative plate motion (70–90%) is indeed accommodated along the main plate boundary faults (Cascadia and Alaska subduction zones, Queen Charlotte–Fairweather transform, Yakutat collision zone). However, a significant portion (10–30%) is accommodated by internal shortening, shear, and block motion within the Cordillera.

The first-order tectonics of the Canada–Alaska Cordillera can be explained simply by a dynamic model accounting for lithosphere strength variations, boundary forces, and gravitational forces related to topography and lithosphere density variations. We argue that because of the very-high-temperature geotherms, most of the Cordillera can be viewed as an orogenic float where the upper crust is mechanically decoupled from the lower part of the lithosphere [e.g., Oldow *et al.*, 1990]. This decoupling facilitates strain transfer and coeval deformation across the Cordillera [e.g., Mazzotti and Hyndman, 2002]. The main exceptions to the orogenic float model are the forearc (and paleo-forearc) regions along the western margin, which are associated with low-temperature profiles. These regions tend to behave primarily as rigid blocks migrating along the plate boundary faults in response to plate boundary dextral shear (Oregon block and possibly Queen Charlotte–Panhandle block) or to lateral extrusion from the Yakutat collision zone (Alaska forearc).

In most of the Canadian Cordillera, tensile gravitational forces are balanced by NE–SW boundary compression [Humphreys and Coblenz, 2007]. Despite the high gravitational forces, extension and collapse are prevented by the lack of “tectonic open end” along the western margin [e.g., Rey *et al.*, 2001]. In contrast, the “tectonic open ends” created by strong slab pull in the southern Cascadia and central Alaska subduction zones [Humphreys and Coblenz, 2007] allow gravitational forces to drive extension and lateral extrusion in the central Alaska and Basin and Range regions.

The most significant tectonic feature of the Canada–Alaska Cordillera is the ongoing collision between the Yakutat block and the Cordillera in the corner of the Gulf of Alaska. The current tectonics in the 1500 × 1000-km region from eastern Yukon to central Alaska can be largely explained by the impact of the collision. As shown in Plate 7, strong boundary compression, and possibly high-tensile gravitational forces, in the St. Elias and eastern Chugach Mountains likely result in northeastward diversion of the Queen Charlotte–Fairweather northward motion; northeastward and northward translation of the central Yukon and active deformation in the Mackenzie and Richardson Mountains; and westward extrusion of the Alaska forearc and eastern-central Alaska regions.

This first-order tectonic–dynamic model can be used to provide quantitative constraints to seismic hazard assessments in the Cordillera. Crustal strain rates derived from a tectonic model or directly from GPS measurements can be used as independent constraints on earthquake statistics and probabilistic seismic hazard models [e.g., Frankel *et al.*, 2002; Mazzotti *et al.*, 2005]. As an example, we present a simple map of $M_w = 7$ earthquake return periods derived from our tectonic model. Although it encompasses large uncertainties, this map points out regions where the geodetic–tectonic model is consistent with the earthquake catalog [e.g., Puget–Georgia Lowland, Hyndman *et al.*, 2003] and regions with significant inconsistencies. The Queen Charlotte margin, inboard of the main Queen Charlotte Fault, is a prime example of a problematic area. Our tectonic model suggests an overall return period of ~15 years in this region, based on a dextral shear rate of ~5 mm/a, whereas the earthquake catalog lacks any such event in the last 100 years. This problem clearly shows that more work is required to understand the relationship between crustal strain and seismic strain but also shows that earthquake catalogs may be limited in their delineation of high seismic hazard zones, especially in areas possibly affected by infrequent characteristic large events.

APPENDIX A: GRAVITATIONAL POTENTIAL ENERGY

We estimate the variations of gravitational potential energy based on average cross-section profiles in the four main tectonic domains (south, central, north, and Alaska). For simplicity, the profiles are divided into five individual columns representing the main structural zones (Figure A1). For the south, central, and Alaska profiles, we define the Insular Belt (forearc and paleo-forearc), Coast Belt (Coast Mountains and western Chugach Mountains–Alaska Range), Central Plateau, Foreland Belt (Rocky Mountains, Mackenzie Mountains, Brooks Range), and Interior Plains columns based on topography and crustal structure characteristics. To a first order, these columns follow the actual geologic belts with the exception of the Central Plateau column, which is defined as the relatively low elevation flat area between the Coast Mountains and Foreland Belt. For the North profile, the two westernmost columns are defined as the Yakutat Block and the Collision Zone (eastern Chugach–St. Elias Mountains).

Under the assumption of local isostatic equilibrium, the gravitational force (F_G) that two columns A and B apply to one another is the difference in gravitational potential energy:

$$F_G = \left[\int_L^S \left(\int_z^S \rho(z') g dz' \right) dz \right]_A - \left[\int_L^S \left(\int_z^S \rho(z') g dz' \right) dz \right]_B,$$

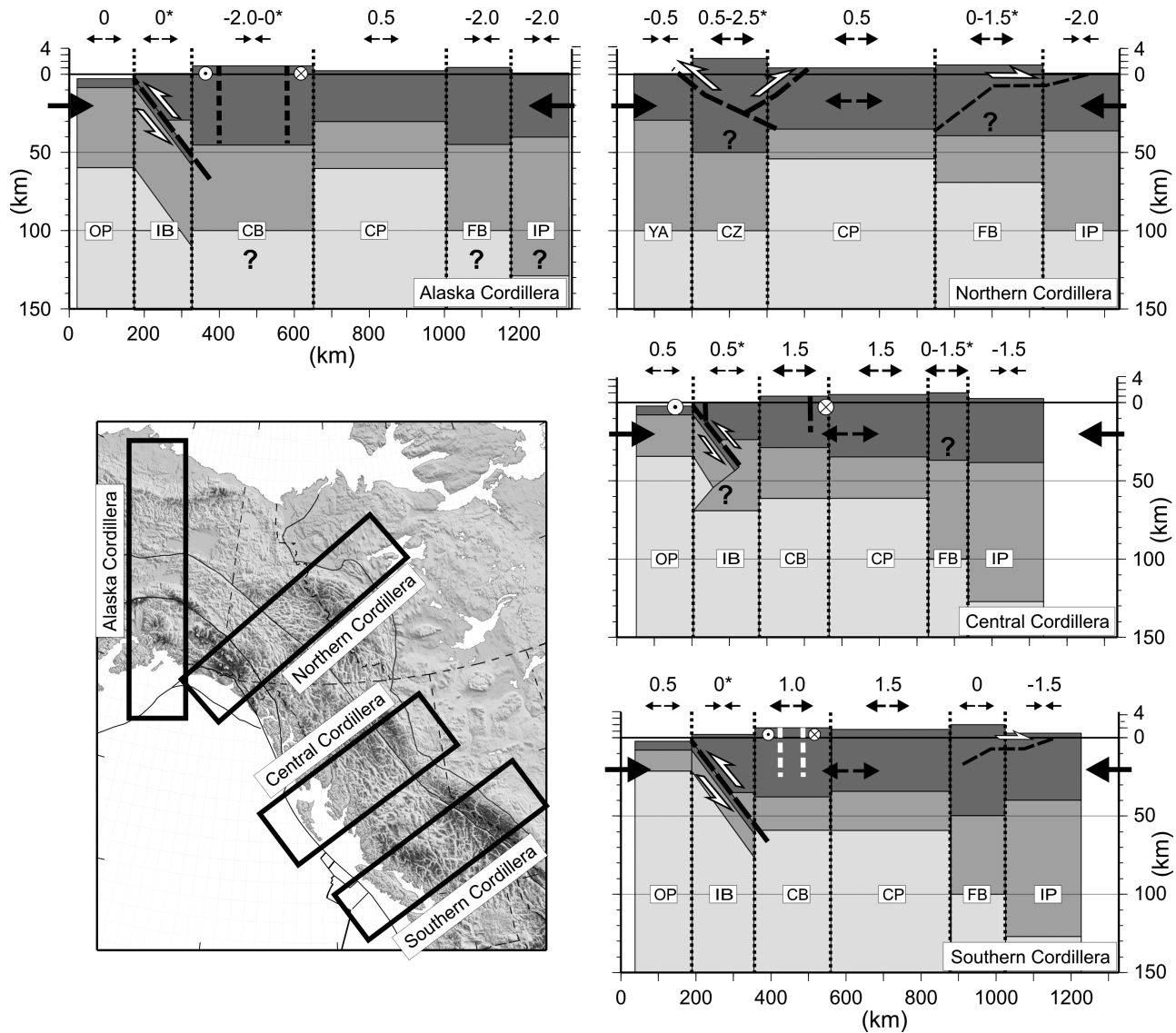


Figure A1. Gravitational force (F_G) across the Cordillera. F_G variations for schematic columns along four cross sections across southern, central, northern, and Alaska tectonic domains. Tension and compression forces are shown by diverging and converging arrows above columns. Large and small arrows indicate values of F_G larger and smaller than integrated lithosphere strength, respectively. F_G values with asterisks are poorly resolved. Dark, medium, and light gray shades indicate crust, lithosphere mantle, and asthenosphere, respectively. CB, Coast Belt; CP, central plateau; CZ, collision zone; FB, Foreland Belt; IB, Insular Belt; IP, interior plains; OP, oceanic plate; YA, Yakutat block.

where $\rho(z)$ is the density profile, g is the gravity acceleration, S is the topography elevation, L is the compensation depth, and z' is an integration variable [e.g., *Molnar and Lyon Caen*, 1988; *Jones et al.*, 1996; *Rey et al.*, 2001]. Details of the parameters used in our calculations are described below and in Table A1:

1. F_G is calculated with respect to an isostatic and mechanical reference column defined as a mid-ocean ridge (asthenosphere section with 3.6 km of water above it; *Rey et al.*, 2001).
2. Topography profiles are based on a 100-km Gaussian filtering of a 2-minute resolution digital elevation model

Table A1. Parameters for Gravitational Force Calculations^a

Profile	Column	S , km	H_C , km	H_L , km	T_M , °C	F_G , 10 ¹² N/m
Southern Cordillera	Insular Belt	0.5	35	130	500	0 ^b
	Coast Belt	1.5	38	60	900	1.0
	Central Plateau	1.3	35	60	800	1.5
	Foreland Belt	2	50	100	600	0
	Interior Plain	0.6	40	130	500	-1.5
Central Cordillera	Insular Belt	0	25	70	700	0.5 ^b
	Coast Belt	1	30	60	800	1.5
	Central Plateau	1.3	35	60	800	1.5
	Foreland Belt	1.5	38	100	600	0–1.5 ^b
	Interior Plain	0.6	40	130	500	-1.5
Northern Cordillera	Yakutat Block	0	30	100	600	-0.5
	Collision Zone	2.5	50	100	800	0.5–2.5 ^b
	Central Plateau	1	35	55	900	0.5
	Foreland Belt	1.5	38	70	800	0–1.5 ^b
	Interior Plain	0.2	36	100	600	-2.0
Alaska Cordillera	Insular Belt	0	30	100	500	0 ^b
	Coast Belt	1.2	45	100	600	-2.0–0 ^b
	Central Plateau	0.5	30	60	800	0.5
	Foreland Belt	0.9	45	100	600	-2.0
	Interior Plain	0.3	40	130	500	-2.0

^a S , topograph elevation; H_C , depth to crust–mantle boundary (Moho); H_L , depth to lithosphere–asthenosphere boundary; T_M , temperature at Moho; F_G , gravitational force. ^b Poorly constrained or potentially biased F_G estimates.

(ETopo2). For each profile, three filtered topography cross sections ~100 km apart (Figure A1) are extracted and averaged to define the mean topography elevation (S) over the regions represented by individual columns.

3. Crustal thicknesses H_C are based on seismic reflection, seismic refraction, receiver function, and gravity data [cf. Cook, 1995; Clowes *et al.*, 1995, 2005; Perry *et al.*, 2002; Veenstra *et al.*, 2006; Fuis *et al.*, 2006; and references therein].
4. Density–depth profiles are defined by dividing the columns into four segments (upper crust, lower crust, lithosphere mantle, and asthenosphere mantle) with average densities based on a thermal expansion and compressibility:

$$\rho(P, T) = \rho_0(1 - \alpha T)(1 + \beta P),$$

where T and P are the average temperature and pressure of the segments and ρ_0 is a reference density at 0°C and 0 km depth: ρ_0 (upper crust) = 2850 kg/m³, ρ_0 (lower crust) = 2950 kg/m³, ρ_0 (lithosphere mantle) = 3360 kg/m³, ρ_0 (asthenosphere mantle) = 3390 kg/m³. Thermal expansion α and compressibility β are assumed constant: $\alpha = 3.1 \times 10^{-5} \text{C}^{-1}$, $\beta = 7.7 \times 10^{-3} \text{GPa}^{-1}$. Density estimates thus require an estimate of the geotherm in each column. We use a simple approximation in which the geotherm is described by three linear segments: from 0°C to T_M in the crust (T_M , temperature at the Moho), from T_M to 1300°C at the

base of the lithosphere (H_L), and an adiabatic gradient in the asthenosphere. The temperature at the Moho (T_M) and the depth corresponding to the base of the thermal lithosphere (H_L) are based on local heat flow and seismic velocity studies [cf. Lewis *et al.*, 2003; Currie and Hyndman, 2006; and reference therein].

Significant sources of uncertainties are the following:

1. The pressure–temperature density profiles in the crust and the mantle are only valid to a first order and do not account for local variations in density attributed to lithologic contrasts. Variations of ~50 kg/m³ in the lithosphere mantle density would result in changes of $\sim 0.5 \times 10^{12} \text{ N/m}$ in F_G [Jones *et al.*, 1996].
2. The crustal thickness, although well defined by seismic data in most regions, is not resolved in the Northern Rocky, Mackenzie, and St. Elias mountains. For the St. Elias Mountains, the lack of constraint on the crustal thickness results in a large range of possible F_G (0.5×10^{12} to $2.5 \times 10^{12} \text{ N/m}$).
3. The assumption of isostatic equilibrium is obviously incorrect in areas where boundary forces are involved in supporting the local topography: the forearc of the Cascadia and Alaska subduction zones, the Yakutat collision zone, and possibly the Queen Charlotte margin where incipient underthrusting is suspected. This limitation also probably applies to the Alaska Coast Belt column, which may be affected by flat subduction of

the Yakutat block. For these columns, the estimated F_G is biased, but the extent of this bias is difficult to estimate without a detailed study of local force balances.

- Most of the columns are near isostatic equilibrium, mostly owing to thermal expansion balancing the high topography/thin crust of the Cordillera and the low topography/thick crust of the Interior Plains [Hyndman and Lewis, 1999]. However, simple pressure–temperature density profiles do not always lead to isostatic equilibrium. For example, the Alaska Foreland Belt elevation appears to be too low compared to the cold thick crustal root of the Brooks Range. The resulting large gravitational compression (Table A1) points to possible issues in some of our assumptions.

Acknowledgments. The authors thank J. Freymueller, D. Scholl, C. Larsen, and J. Townend for their constructive reviews and comments. This synthesis benefited from several University of Victoria Ph.D. projects as well as discussions with H. Dragert, K. Wang, and A. Frederiksen. GPS data are from the Canadian Crustal Deformation Service, BC Base Mapping and Geomatic Services, Alaska Deformation Array, U.S. Continuously Operating Reference Stations, and Canadian Base Network. Figures are partly made with the GMT software [Wessel and Smith, 1995]. Geological Survey of Canada contribution 20070423.

REFERENCES

- Adams, J., and S. Halchuk (2003), Fourth generation seismic hazard maps of Canada: Values for over 650 Canadian localities intended for the 2005 Building Code of Canada, *Geol. Surv. Can. Open File*, 4459.
- Altamimi, Z., P. Sillard, and C. Boucher (2002), ITRF2000: A new release of the International Terrestrial Reference Frame for earth science applications, *J. Geophys. Res.*, *107*(B10), 2214, doi:10.1029/2001JB000561.
- Blackwell, D. D., and M. C. Richards (2004), *Geothermal Map of North America*, scale 1:6,500,000, AAPG product code 423, Am. Assoc. of Pet. Geol., Tulsa, Okla. (Available at: <http://www.smu.edu/geothermal/2004NAMap/2004NAMap.htm>)
- Bustin, A. M. (2006), The thermal structure, deformation from GPS, and seismicity related to oblique convergence along the Queen Charlotte margin, British Columbia, Ph.D. thesis, Univ. of Victoria, Victoria, B. C., Canada.
- Cassidy, J. F., R. M. Ellis, C. Karavas, and G. C. Rogers (1998), The northern limit of the subducted Juan de Fuca plate system, *J. Geophys. Res.*, *103*, 26,949–26,961.
- Cassidy, J. F., G. C. Rogers, and J. Ristau (2005), Seismicity in the vicinity of the SNORCLE corridors of the northern Canadian Cordillera, *Can. J. Earth Sci.*, *42*, 1137–1148.
- Clowes, R. M., C. A. Zelt, J. R. Amor, and R. E. Ellis (1995), Lithospheric structure in the southern Canadian Cordillera from a network of seismic refraction lines, *Can. J. Earth Sci.*, *32*, 1485–1513.
- Clowes, R. M., P. T. C. Hammer, G. F. Viego, and J. K. Welford (2005), Lithospheric structure in northwestern Canada from LITHOPROBE seismic refraction and related studies: A synthesis, *Can. J. Earth Sci.*, *42*, 1277–1293.
- Colpron, M., J. L. Nelson, and D. C. Murphy (2007), Northern Cordilleran terranes and their interactions through time, *GSA Today*, *17*, doi:10.1130/GSAT01704-5A.1.
- Cook, D. G. (1991), Mackenzie mountains, Franklin mountains and Colville hills: Structural styles, in *Geology of the Cordilleran orogen in Canada*, vol. G2, edited by H. Gabrielse and C. J. Yorath and compiled by H. Gabrielse, pp. 571–675, Geol. Soc. of Am., Boulder, Colo.
- Cook, F. A. (1995), The reflection Moho beneath the southern Canadian Cordillera, *Can. J. Earth Sci.*, *32*, 1520–1530.
- Currie, C. A., and R. D. Hyndman (2006), The thermal structure of subduction zone back arcs, *J. Geophys. Res.*, *111*, B08404, doi:10.1029/2005JB004024.
- DeMets, C., R. G. Gordon, D. F. Argus, and S. Stein (1990), Current plate motions, *Geophys. J. Int.*, *101*, 425–478.
- Dragert, H., K. Wang, and T. S. James (2001), A silent slip event on the deeper Cascadia subduction interface, *Science*, *292*, 1525–1528.
- Flesch, L. M., W. E. Holt, A. J. Haines, and B. Sheng-Tu (2000), Dynamics of the Pacific–North America plate boundary in the western United States, *Science*, *287*, 834–836.
- Fletcher, H. J. (2002), Crustal deformation in Alaska measured using the Global Positioning System, Ph.D. thesis, Univ. of Alaska, Fairbanks.
- Fletcher, H. J., and J. T. Freymueller (2003), New constraints on the motion of the Fairweather Fault, Alaska, from GPS observation, *Geophys. Res. Lett.*, *30*(3), 1139, doi:10.1029/2002GL016476.
- Flück, P., R. D. Hyndman, and C. Lowe (2003), Effective elastic thickness T_e of the lithosphere in western Canada, *J. Geophys. Res.*, *108*(B9), 2430, doi:10.1029/2002JB002201.
- Frankel, A. D., M. D. Petersen, C. S. Mueller, K. M. Haller, R. L. Wheeler, E. V. Leyendecker, R. L. Wesson, S. C. Harmsen, C. H. Cramer, D. M. Perkins, and K. S. Rukstales (2002), Documentation for the 2002 update of the national seismic hazard maps, *U.S. Geol. Surv. Open File Rep.*, 02-420.
- Freed, A. M., R. Bürgmann, E. Calais, J. Freymueller, and S. Hreinsdóttir, (2006), Implications of deformation following the 2002 Denali, Alaska, earthquake for postseismic relaxation processes and lithosphere rheology, *J. Geophys. Res.*, *111*, B01401, doi:10.1029/2005JB003894.
- Freymueller, J. T., S. C. Cohen, and H. J. Fletcher (2000), Spatial variations in present-day deformation, Kenai Peninsula, Alaska, and their implications, *J. Geophys. Res.*, *105*, 8079–8101.
- Fuis, G. S., T. E. Moore, B. C. Beaudoin, T. M. Brocher, N. I. Christensen, M. A. Fisher, A. R. Levander, W. J. Nokleberg, R. A. Page, and G. Plafker (2006), Crustal evolution as seen in a transect across Alaska, from Pacific to Arctic margins, *Geol. Soc. Am. Abstr.*, *38*(5), 80.
- Gabrielse, H. (1991), Structural styles, in *Geology of the Cordilleran orogen in Canada*, edited by H. Gabrielse and C. J. Yorath, *Geol. North Am.*, *G2*, 571–675.

- Glen, J. M. G. (2004), A kinematic model for the southern Alaska orocline based on regional fault patterns, in *Orogenic Curvature*, edited by A. Sussman and A. B. Weil, *Spec. Pap. Geol. Soc. Am.*, 383, 161–173.
- Haeussler, P. J., D. C. Bradley, R. E. Wells, and M. L. Miller (2003), Life and death of the Resurrection plate: Evidence for its existence and subduction in the northeastern Pacific in Paleocene–Eocene time, *Geol. Soc. Am. Bull.*, 115, 7, 867–880.
- Hreinsdóttir, S., J. T. Freymueller, R. Bürgmann, and J. Mitchell (2006), Coseismic deformation of the 2002 Denali Fault earthquake: Insight from GPS measurements, *J. Geophys. Res.*, 111, B03308, doi:10.1029/2005JB003676.
- Humphreys, E. D., and D. D. Coblenz (2007), North American dynamics and western U.S. tectonics, *Rev. Geophys.*, 45, RG3001, doi:10.1029/2005RG000181.
- Hyndman, R. D., and T. S. Hamilton (1993), Queen Charlotte area Cenozoic tectonics and volcanism and their association with relative plate motion along the northeastern Pacific margin, *J. Geophys. Res.*, 98, 14,257–14,277.
- Hyndman, R. D., and T. J. Lewis (1999), Geophysical consequences of the Cordillera–Craton thermal transition in southwestern Canada, *Tectonophysics*, 306, 397–422.
- Hyndman, R. D., and D. H. Weichert (1983), Seismicity and rates of relative motion on the plate boundaries of western North America, *Geophys. J. Int.*, 72, 59–82.
- Hyndman, R. D., S. Mazzotti, D. Weichert, and G. C. Rogers (2003), Frequency of large crustal earthquakes in Puget Sound–Southern Georgia Strait predicted from geodetic and geological deformation rates, *J. Geophys. Res.*, 108(B1), 2033, doi:10.1029/2001JB001710.
- Hyndman, R. D., C. Currie, and S. Mazzotti (2005a), Subduction zone backarcs, mobile belts, and orogenic heat, *Geol. Soc. Am. Today*, 15, doi:10.1130/1052-5173.
- Hyndman, R. D., P. Flück, S. Mazzotti, T. Lewis, J. Ristau, and L. Leonard (2005b), Current tectonics of the Northern Canadian Cordillera, *Can. J. Earth Sci.*, 42, 1117–1136, doi:10.1139/E05-023.
- Jackson, J. (2002), Strength of the continental lithosphere: Time to abandon the jelly sandwich?, *Geol. Soc. Am. Today*, 10, 4–10.
- Jones, C. H., J. R. Unruh, and L. J. Sonder (1996), The role of gravitational potential energy in active deformation in the southwestern United States, *Nature*, 381, 37–41.
- Kohlstedt, D. L., B. Evans, and S. J. Mackwell (1995), Strength of the lithosphere: Constraints imposed by laboratory experiments, *J. Geophys. Res.*, 100, 17,587–17,602.
- Kreemer, C., W. E. Holt, and A. J. Haines (2003), An integrated global model of present-day plate motions and plate boundary deformation, *Geophys. J. Int.*, 154, 8–34.
- Larsen, C. F., R. J. Motyka, J. T. Freymueller, K. A. Echelmeyer, and E. R. Ivins (2005), Rapid viscoelastic uplift in southeast Alaska caused by post-Little Ice Age retreat, *Earth Planet. Sci. Lett.*, 237, 548–560.
- Leonard, L. J. (2006), GPS and seismicity constraints on the current tectonics of the northern Canadian Cordillera, Ph.D. thesis, Univ. of Victoria, Victoria, B. C., Canada.
- Leonard, L. J., R. D. Hyndman, S. Mazzotti, L. L. Nykolaishen, M. Schmidt, and S. Hippchen (2007), Current deformation in the northern Canadian Cordillera inferred from GPS measurements, *J. Geophys. Res.*, 112, B11401, doi:10.1029/2007JB005061.
- Lewis, T. J., C. Lowe, and T. S. Hamilton (1997), Continental signature of a ridge–trench–triple junction: Northern Vancouver Island, *J. Geophys. Res.*, 102, 7767–7782.
- Lewis, T. J., R. D. Hyndman, and P. Flück (2003), Heat flow, heat generation, and crustal temperatures in the northern Canadian Cordillera: Thermal control of tectonics, *J. Geophys. Res.*, 108(B6), 2316, doi:10.1029/2002JB002090.
- McCaffrey, R., M. D. Long, C. Goldfinger, P. C. Zwick, J. L. Nabeleck, C. K. Johnson, and C. Smith (2000), Rotation and plate locking along the southern Cascadia subduction zone, *Geophys. Res. Lett.*, 27, 3117–3120.
- McCaffrey, R., A. I. Qamar, R. W. King, and R. Wells (2006), Plate coupling, block rotation and crustal deformation in the Pacific Northwest, *Eos Trans. AGU*, 87, Fall Meet. Suppl., Abstract G41A-08.
- Mazzotti, S., and J. Adams (2005), Rates and uncertainties on seismic moment and deformation rates in eastern Canada, *J. Geophys. Res.*, 110, B09301, doi:10.1029/2004JB003510.
- Mazzotti, S., and R. D. Hyndman (2002), Yakutat collision and strain transfer across the northern Canadian Cordillera, *Geology*, 30, 495–498.
- Mazzotti, S., H. Dragert, R. D. Hyndman, M. M. Miller, and J. A. Henton (2002), GPS deformation in a region of high crustal seismicity: N. Cascadia forearc, *Earth Planet. Sci. Lett.*, 198, 41–48.
- Mazzotti, S., H. Dragert, J. Henton, M. Schmidt, R. D. Hyndman, T. James, Y. Lu, and M. Craymer (2003a), Current tectonics of northern Cascadia from a decade of GPS measurements, *J. Geophys. Res.*, 108(B12), 2554, doi:10.1029/2003JB002653.
- Mazzotti, S., R. D. Hyndman, P. Flück, A. J. Smith, and M. Schmidt (2003b), Distribution of the Pacific–North America motion in the Queen Charlotte Islands–S. Alaska plate boundary zone, *Geophys. Res. Lett.*, 30(14), 1762, doi:10.1029/2003GL017586.
- Mazzotti, S., T. S. James, J. Henton, and J. Adams (2005), GPS crustal strain, postglacial rebound, and seismicity in eastern North America: The Saint Lawrence valley example, *J. Geophys. Res.*, 110, B11301, doi:10.1029/2004JB003590.
- Miller, M. M., D. J. Johnson, C. M. Rubins, H. Dragert, K. Wang, A. Qamar, and C. Goldfinger (2001), GPS-determination of along-strike variation in Cascadia margin kinematics: Implication for relative plate motion, subduction zone coupling, and permanent deformation, *Tectonics*, 20, 161–176.
- Molnar, P., and H. Lyon Caen (1988), Some simple physical aspects of the support, structure, and evolution of mountains belts, *Spec. Pap. Geol. Soc. Am.*, 218, 179–207.
- Monger, J. W. H., and R. A. Price (2002), The Canadian Cordillera: Geology and tectonic evolution, *CSEG Rec.*, 17–36, February.
- Ohta, Y., J. T. Freymueller, S. Hreinsdóttir, and H. Suito (2006), A large slow slip event at the depth of the seismogenic zone in the south central Alaska subduction zone, *Earth Planet. Lett.*, 247, 108–116.

- Oldow, J.S., A. W. Bally, and H. G. Ave Lallemand (1990), Transpression, orogenic float, and lithospheric balance, *Geology*, *18*, 991–994.
- Page, R. A., G. Plafker, and H. Pulpan (1995), Block rotation in east-central Alaska: A framework for evaluating earthquake potential?, *Geology*, *23*, 629–632.
- Perry, H. K. C., D. W. S. Eaton, and A. M. Forte (2002), LITH5.0: A revised crustal model for Canada based on LITHOPROBE results, *Geophys. J. Int.*, *150*, 285–294.
- Plafker, G., and H. C. Berg (1994), Overview of the geology and tectonic evolution of Alaska, in *Geology of Alaska, Geology of North America*, edited by G. Plafker and H. C. Berg, *Decade of North American Geology*, vol. G1, pp. 989–1021, Geol. Soc. of Am., Boulder, Colo.
- Plafker, G., L. M. Gilpin, and J. C. Lahr (1994), Neotectonic map of Alaska, in *Geology of Alaska, Geology of North America*, edited by G. Plafker and H. C. Berg, *Decade of North American Geology*, vol. G2, plate 12, 1 sheet, 1:2,500,000 scale, Geol. Soc. of Am., Boulder, Colo.
- Ranalli, G. (1995), *Rheology of the Earth*, 2nd ed., p. 413, CRC Press, London.
- Redfield, T. F., and P. G. Fitzgerald (1993), Denali fault system of southern Alaska: An interior strike-slip structure responding to dextral and sinistral shear coupling, *Tectonics*, *12*, 1195–1208.
- Redfield, T. F., D. W. Scholl, M. E. Beck, and P. G. Fitzgerald (2006), The extrusion of Alaska: Past, present, and future, *Eos Trans. AGU*, *87*, Fall Meet. Suppl., Abstract T43D-1682.
- Rey, P., O. Vanderhaeghe, and C. Teyssier (2001), Gravitational collapse of the continental crust: Definition, regimes and modes, *Tectonophysics*, *342*, 435–449.
- Ristau, J., G. C. Rogers, and J. F. Cassidy (2007), Stress in western Canada from regional moment tensor analysis, *Can. J. Earth Sci.*, *44*, 127–148.
- Sauber, J., S. McClusky, and R. King (1997), Relation of ongoing deformation rates to the subduction zone process in southern Alaska, *Geophys. Res. Lett.*, *24*, 2853–2856.
- Smith, A. J., R. D. Hyndman, J. F. Cassidy, and K. Wang (2003), Structure, seismicity, and thermal regime of the Queen Charlotte Transform Margin, *J. Geophys. Res.*, *108*(B11), 2539, doi:10.1029/2002JB002247.
- Stein, S., and J. T. Freymueller (Eds.) (2002). *Plate Boundary Zones*, *Geodyn. Ser.*, vol. 30, 425 pp., AGU, Washington, D.C.
- Thatcher, W. (2003), GPS constraints on the kinematics of continental deformation, *Int. Geol. Rev.*, *45*, 191–2212.
- Townend, J., and M. D. Zoback (2000), How faulting keeps the crust strong, *Geology*, *5*, 399–402.
- van der Lee, S., and A. Frederiksen (2005), Surface wave tomography applied to the North American upper mantle, in *Seismic Earth: Array Analysis of Broadband Seismograms*, *Geophys. Monogr., Ser.*, vol. 157, edited by A. Levander and G. Nolet, pp. 67–80, AGU, Washington, D.C.
- Veenstra, E., D. H. Christensen, G. A. Abers, and A. Ferris (2006), Crustal thickness variations in south-central Alaska, *Geology*, *34*, 9, doi:10.1130/G22615.1.
- Wang, K., R. Wells, S. Mazzotti, R. D. Hyndman, and T. Sagiya (2003), A revised dislocation model of interseismic deformation of the Cascadia subduction zone, *J. Geophys. Res.*, *108*(B1), 2026, doi:10.1029/2001JB001227.
- Wells, D. L., and K. J. Coppersmith (1994), New empirical relationships among magnitude, rupture length, rupture width, rupture area, and surface displacement, *Bull. Seismol. Soc. Am.*, *84*, 974–1002.
- Wells, R. E., C. S. Weaver, and R. J. Blakely (1998), Forearc migration in Cascadia and its neotectonic significance, *Geology*, *26*, 759–762.
- Wessel, P., and W. H. F. Smith (1995), New version of the Generic Mapping Tools released, *EOS Trans. AGU*, *76*, Fall Meet. Suppl., F329.
- Whittaker, A., M. H. P. Bott, and G. D., Waghorn (1992), Stresses and plate boundary forces associated with subduction plate margins, *J. Geophys. Res.*, *97*, 11,933–11,944.
- Zoback, M. L. (1992), First and second-order patterns of stress in the lithosphere: The World Stress Map project, *J. Geophys. Res.*, *97*, 11,703–11,728.
- Zoback, M. D., and M. L. Zoback (1991), Tectonic stress field of North America and relative plate motions, in *Neotectonics of North America*, edited by D. B. Slemmons, E. R. Engdahl, M. D. Zoback, and D. D. Blackwell, *Decade of North American Geology*, vol. 1, Geol. Soc. of Am., Boulder, Colo.
- Zoback, M. D., J. Townend, and B. Grollimund (2002), Steady-state failure equilibrium and deformation of intraplate lithosphere, *Int. Geol. Rev.*, *44*, 383–401.
- Zweck, C., J. T. Freymueller, and S. C. Cohen (2002), Three-dimensional elastic dislocation modeling of the postseismic response to the 1964 Alaska earthquake, *J. Geophys. Res.*, *107*(B4), 2064, doi:10.1029/2001JB000409.

J. F. Cassidy, R. D. Hyndman, L. J. Leonard, and S. Mazzotti, Geological Survey of Canada, Natural Resources Canada, 9860 West Saanich Road, Sidney, BC, Canada V8L 4B2, and School of Earth and Ocean Science, University of Victoria, Victoria, BC, Canada V8W 3P6.

